AD-A009 863

THE MECHANICAL BEHAVIOR OF POLY(METHYL METHACRYLATE) UNDER PRESSURE

K. Matsushige, et al

Case Western Reserve University

Prepared for:

Office of Naval Research

3 February 1975

DEPARTMENT OF MACROMOLECULAR SCIENCE

SCHOOL OF ENGINEERING

CASE INSTITUTE OF TECHNOLOGY
OF
CASE WESTERN RESERVE UNIVERSITY

THE MECHANICAL BEHAVIOR OF

POLY(METHYL METHACRYLATE) UNDER PRESSURE

by

K. Matsushige*, S. V. Radcliffe+ and E. Baer*
*Department of Macromolecular Science
+Department of Metallurgy and Material Science
Case Western Reserve University
Cleveland, Ohio 44106

N0014-69-A-0404-0013
NR-039-120

T.R. No. 270

February 3, 1975

SYNOPSIS

Tensile deformation of poly(methyl methacrylate) carried out under hydrostatic pressure up to 4 kb has shown that the pressure-transmitting fluid (silicon oil) strongly affects the mechanical properties of this polymer. Unsealed specimens fractured in a brittle manner at almost the same strain of 5% in the whole pressure range examined, while specimens sealed with Teflon tape and rubber showed a brittle to ductile transition at only 0.25 kb. At this pressure, the craze initiation and shear band initiation stresses were found to become equal. The pressure dependency of the shear band initiation stress could be expressed well with a "non-linear" pressure dependent von Mises criterion and the onset of the shear banding was proved to relate to the enthalpy energy density stored in the specimen. The combination of the non-linear pressure dependent von Mises criterion and the enthalpy energy density concept enabled us to predict the pressure dependency of Young's modulus.

INTRODUCTION

Hydrostatic pressure has been shown to cause significant effects on the mechanical properties of polymers. The change in fracture modes from brittle to ductile in tensile deformation has been reported for a few amorphous polymers such as polystyrene (PS)[1-4], polyimide (PI)[5], and polysulfone (PSF)[6]. In the preceeding paper[4], we have observed that the brittle to ductile transition in PS, which was previously reported to occur at about 2.8 kb[2,3], appears at only 0.35 kb if the environmental effect due to a pressure-transmitting fluid is prevented.

The mechanical behavior of poly(methyl methacrylate) (PMMA) has been investigated under a wide range of pressure by several research groups[3, 7-9] but, to date, such a brittle to ductile transition has not been observed up to the maximum pressure examined, 7.7 kb. In this previous work, however, the environmental effects on the mechanical behavior of PMMA received surprisingly little attention.

The increase in the yield stress of polymers under pressure has also received considerable attention because there is a large effect. To take the significant pressure dependency of yield stress into account, modifications of simple non-pressure dependent yield criteria such as the Tresca and the von Mises, have been attempted in several ways[10-14]. One of the most successful pressure modified criteria seems to be a "linear" pressure dependent von Mises criterion[13]. Recent studies[4,14], however, demonstrated that this criterion agrees well with the experimental only in the lower pressure range and that a "non-linear" pressure dependent von Mises criterion[15] gives better agreement with the data in the whole pressure range. Thus, it has been possible to predict the pressure dependency of yield stress of polymers, but we still lack a more fundamental understanding of the yielding process

under pressure or of why the hydrostatic pressure causes such a significant increase in yield stresses of polymers.

Attempts also have been made to account for the increase of Young's modulus with pressure. Sauer et al.[16-18] suggested that the Birch modification[19] of the Murnaghan finite-strain theory[20] predicts the pressure dependency of Young's modulus for various polymers with close agreement. This theory, however, is reported to fail in the prediction of shear modulus under pressure[21].

The purposes of this paper are to examine whether PMMA also exhibits the brittle to ductile transition under pressure if the possible environmental effects are prevented and to investigate the mechanism for the transition. Further attempts are made to present a thermodynamic understanding of the shear banding phenomenon under pressure and a more acceptable equation for the pressure dependence of Young's modulus.

EXPERIMENTAL

High Pressure Tensile Measurements

The material (PMMA) studied in this work was obtained commercially in the form of a 0.50 in. diameter rod from Cadillac Plastic and Chemical Co.. The tensile specimens for high pressure experiments were machined directly from the rod and the surface was carefully polished along the gauge length. The overall specimen length was 2.40 in. and the reduced gauge section with 1.50 in. R groove was 0.12 in. in diameter. In order to prevent possible environmental effects, the surface of the gauge section was sealed with Teflon tape and transparent silicon rubber (RTV 108 from General Electric). A detailed discussion of necessary corrections to obtain true stress-strain curves, together with an account of the high pressure-tensile test apparatus used in this study, has been given elsewhere[4]. The tensile tests were conducted at a constant strain rate of 1.30 $\pm$ 0.15%/min and at room temperature of 23 $\pm$ 1°C; silicon oil (Dow Corning 200 Fluids, 500 cs) was used as the pressure transmitting fluid.

Optical Measurements

The optical observation of crazing and/or shear banding and the measurement of stress-strain behavior were simultaneously carried out at atmospheric pressure using the facilities composed of a Tensilon UTM-II (Toyo Measuring Instruments Co.) on which a polarizing microscope was mounted[22]. For the optical observation, flat tensile specimens were hot-molded from the same rod described above. The resulting specimen was almost completely stain-free, as determined by examination in polarized light. The specimen measured approximately 0.02 in. thickness and 0.75 in.

R groove and 0.05 in. width at the center.

Compression Measurements

Compressive shear band initiation and yielding stresses were measured with an Instron testing machine using a cylindrical specimen. The specimen was cut from the rod and had a geometry of about 0.2 in. in diameter and 0.5 in. in height. The tests were carried out under almost the same conditions of temperature and strain rate conditions as those of the high pressure tensile tests.

RESULTS AND ANALYSIS

Mechanism of Brittle to Ductile Transition

Figure 1 shows typical stress-strain curves of unsealed specimens tested at different pressures. Fracture stresses were observed to increase substantially with increasing pressure but all specimens fractured before yielding in a brittle manner at almost the same strain of 5% in the whole pressure range examined. The direction of the fracture surfaces was perpendicular to the tensile direction and the surfaces were very smooth. Closer examination of the fracture surfaces in an optical microscope showed the occurrence of parabolic markings, a characteristic fracture features in PMMA[23-25]. These markings decreased with increasing applied pressure and no such markings could be observed for specimens tested above 1.5 kb. Although the observed fracture stresses, $\sigma_f(P)$, increased with pressure, the values of the principal fracture stresses, $\sigma_f^1(P) = \sigma_f(P) - P$, decreased and became negative above about 1.5 kb, as later shown in Figure 10. This observation suggests an interesting coincidence with the relationship observed from the fracture experiments at atmospheric pressure[26]; the number of the parabolic markings during catastrophic crack propagation decreases by decreasing the fracture stress.

To avoid the environmental effects due to surface contact of specimens with the pressure transmitting fluid (silicon oil), the specimens were sealed with Teflon tape and rubber and tested under the same experimental conditions as those for the unsealed specimens. As shown in Figure 2, the stress-strain curves for the sealed specimens appeared quite differently from those for the unsealed ones. The ductility of the specimens increased substantially with pressure and the specimens fractured after necking in a ductile manner above only 0.3 kb.

To investigate the mechanism for the brittle to ductile transition, optical observations of crazing and/or shear banding and the measurement of stress-strain curves were performed simultaneously. Due to experimental difficulties, flat specimens were mounted in a Tensilon UTM-II tensile tester with a polarizing microscope attachment and tested at atmospheric pressure. Figure 3 shows a stress-strain curve and photographs of the test specimen at various strain levels. The experimental temperature was 25°C, where PMMA fractures in a brittle manner. In the linear region of the stress-strain curve, the specimen deformed uniformly and no craze or shear band could be detected. When the stress-strain curve showed a departure from the linearity, craze initiation was observed. The craze region spread out and the number of crazes increased rapidly with increasing stress. Finally, one of the crazes developed into a major crack leading the specimen to fracture before a yield point was observed. Thus, it is very likely that the onset of nonlinearity on the stress-strain curve is accompanied by craze initiation. A similar relation between the craze initiation and the stress-strain behavior has been reported for other amorphous polymers such as PS[27,28] and polycarbonate (PC)[28].

To study the deformation process in the ductile fracture region, a similar experiment was carried out at 95°C using polarized light. At this high temperature, the craze formation was not observed during the entire deformation process. Birefrigence indicated that shear banding initiated at the stress level corresponding to the inflection point on the stress-strain curve. The birefrigent color zone propagated at an angle of 40°-45° to the tensile deformation direction and fully expanded across the specimen width just before the yield point. Figure 4 shows a typical stress-strain curve and

a series of photographs taken at increasing strains in addition to the schematic representations of the photographic observations.

Our observations on tensile deformation of PMMA are characteristically quite similar to the results of Kramer[29] who while observing PS in compression noted that the shear zone is accompained by non-linearity of the stress-strain curve and also that the propagation of the shear zone contributes to non-Hookean shear strain. The shear zone consists of many individual fine shear bands[30], and the morphologies of these bands in a number polymer systems are the subject of recent studies using electron microscopy[30-32].

As described above, the onset of non-linearity on the stress-strain curves is accompained by craze initiation in the brittle fracture region or by shear band initiation in the ductile fracture region. Therefore, we define the corresponding stresses as the craze initiation and shear band (rather than shear zone) initiation stresses, respectively. The stress-strain curves observed under pressure are analyzed in this way and the various stresses, such as craze initiation, brittle fracture, shear band initiation, and yield stresses, are plotted as a function of the experimental pressure as is shown in Figure 5. The craze initiation stress shows much higher pressure dependency than the shear band initiation stress. These stresses become equal at the pressure where the brittle to ductile transition was observed. Above the transition pressure, the shear bands initiate and propagate in the specimen before crazes can form thus preventing crazing which leads to brittle fracture at low elongation. This mechanism for the brittle to ductile transition is supported by other microscopic studies[33-35] on the

interaction between crazes and shear bands which showed that shear bands function as craze "stoppers" and provide a mechanism for localized strain energy absorption.

Energy Density for Onset of Shear Bands

In this section, the experimental results for shear band initiation and yield stresses are further analyzed. A thermodynamic interpretation which explains the effect of pressure on the onset of shear banding is also presented.

It is instructive to compare the experimental values for the shear band initiation stress and the yield stress with the values predicted from the linear[13] and the non-linear pressure dependent von Mises criteria[15]. The general forms for these criteria in three dimensional stress state can be expressed respectively as follows:

$$[(\sigma_1 - \sigma_2)^2 + (\sigma_2 - \sigma_3)^2 + (\sigma_3 - \sigma_1)^2]^{1/2} + 3\sqrt{2}\,\frac{(C-T)}{(C+T)}\sigma_m = 2\sqrt{2}\,CT \qquad (1)$$

and

$$(\sigma_1 - \sigma_2)^2 + (\sigma_2 - \sigma_3)^2 + (\sigma_3-\sigma_1)^2 + 6\,(C-T)\,\sigma_m = 2CT \qquad (2)$$

where σ_1, σ_2, and σ_3 are the three principal stresses applied to the tensile specimen, $\sigma_m = (\frac{\sigma_1+\sigma_2+\sigma_3}{3})$ is the mean stress, and C and T are the compressive and tensile shear band initiation or yield stresses at atmospheric pressure. We are interested in tensile deformation under hydrostatic pressure, where the three principal stresses are described as $\sigma_1 = \sigma - P$ and $\sigma_2 = \sigma_3 = -P$, and σ is the observed shear band initiation or yield stress under pressure. By

inserting these values into the general equations of (1) and (2), the following normalized expressions[14] for the linear (eq. (3)) and non-linear (eq. (4)) pressure dependent von Mises criteria may be derived;

$$R = 1 + \frac{3}{2} B \left(\frac{X-1}{X}\right) \tag{3}$$

and

$$R = -\frac{X-1}{2} + \frac{1}{2}\left[(X+1)^2 + 12\,B(X-1)\right]^{1/2} \tag{4}$$

where $R = \sigma/T$, $X = C/T$, and $B = P/T$.

To calculate the theoretical values predicted from eqs. (3) and (4), the values of T for shear band initiation and yield were obtained by extrapolating the curves for each process observed under pressure to atmospheric pressure (see Fig. 5) since PMMA is brittle in tension at atmospheric pressure. Values of C can, however, be obtained directly from compression test performed at atmospheric pressure.

As shown in Figure 6, the experimental data for shear banding fit well with the curve predicted from the non-linear pressure dependent von Mises (eq.(4)), suggesting that this criterion, originally derived to explain the yielding, can also be applied without any correction to the shear banding phenomenon. The experimental data for yielding show some discrepancy from the both criteria but indicate a preference for the non-linear criterion at higher pressure region.

We still lack a definitive understanding of why the non-linear pressure dependent von Mises criterion predicts more reasonable behavior than

the linear pressure dependent criterion. These criteria were originally derived simply using mathematical models without any fundamental consideration for the physical processes which control either shear banding or yielding phenomenon. It should be noted that eq. (2), which expresses a paraboloidal surface in three dimensional principal space, is more reasonable because this equation avoids the physically unlikely angular apex of the cone that eq. (1) contains in the first octant of the principal stress space[36].

Recognizing these problems we have attempted to understand from a thermodynamic viewpoint the shear banding or yielding processes under pressure. Figure 7 shows a typical stress-strain curves for ductile fracture; the shear band initiation and yielding points are indicated by arrows. As is well known, the following values can be regarded as the energies per unit volume (energy densities) required for the onset of shear banding and yielding;

$$W_{sb} = \int_0^{\varepsilon_{sb}} \sigma\ (\varepsilon)\ d\varepsilon \tag{5}$$

$$W_y = \int_0^{\varepsilon_y} \sigma(\varepsilon)\ d\varepsilon \tag{6}$$

where ε_{sb} and ε_y are the shear band initiation and yielding strains. The stress-strain curves obtained in this study are analyzed in this way and the calculated values of the energy densities are plotted as a function of experimental pressure in Figure 8. Surprisingly, data for both shear banding

and yielding exhibit good linear pressure dependencies expressed numerically as

$$W_{sb} = 0.18 + 5.0 \times 10^{-3} P \qquad (cal/cm^3) \tag{7}$$

$$W_y = 0.53 + 1.7 \times 10^{-2} P \qquad (cal/cm^3) \tag{8}$$

where the unit of pressure P is cal/cm^3 ($=4.20 \times 10^{-2}$ kb). These facts suggest that the shear banding and yielding phenomena may be simply related to certain thermodynamical function.

The linear pressure dependency of the energy density can be successfully described using an enthalpy energy function. Above the glass transition temperature, amorphous polymers without crosslinks flow uniformly with infinitesimal applied stress. When the state becomes glassy by a lowering of temperature and/or an application of hydrostatic pressure, an additional energy is required to overcome the energy barrier for molecular mobility due to the lowering of the enthalpy energy. This additional enthalpy energy density (ΔH) at the state of temperature T ($<Tg$) and pressure P may be expressed as

$$\Delta H(T,P) = H(Tg,1) - H(T,P)$$

$$= \int_T^{Tg} \int_1^P \frac{\partial^2 H(T,P)}{\partial T \partial P} \, dT \, dP$$

$$\simeq \bar{C}_p \cdot \bar{\rho} \, (Tg - T) + (1 - T \cdot \bar{\alpha})(P - 1) \tag{9}$$

$$\simeq \bar{C}_p \cdot \bar{\rho} \, (Tg - T) + (1 - T \cdot \bar{\alpha})P \quad (\text{For } P \gg 1) \tag{9a}$$

where C_p, ρ, and α are the specific heat capacity at constant pressure, density, and thermal expansion coefficient, respectively, and the upper bars represent the average values of these quantities in the temperature range T to Tq and the pressure range 1 to P. The mechanical energy density W(T,P) due to tensile deformation is converted to energy density which overcomes the activation energy for flow with an efficiency coefficient K, which is a material constant;

$$\Delta H(T,P) = K \cdot W(T,P) \tag{10}$$

By combining eq. (9) with eq. (10), the pressure and temperature dependencies of the mechanical energy density necessary to cause shear banding or yielding are expressed as

$$\left(\frac{\partial W}{\partial P}\right)_T = \frac{1}{K}\left(1 - T \cdot \bar{\alpha}\right) \tag{11}$$

$$\left(\frac{\partial W}{\partial T}\right)_p = -\frac{1}{K}\,\bar{C}_p \cdot \bar{\rho} \tag{12}$$

Eq. (11) suggests that the energy density at constant temperature increases linearly with applied pressure, which is exactly what we observed. Equation (12) suggests that the energy density is a linear temperature function at constant pressure. This prediction agrees well with the experimental results by Macosko and Brand[37] who reported that the tensile yielding energy densities for five amorphous polymers of PMMA, PC, polyacrylsulfone, PSF, and poly(vinyl chloride)tested at atmospheric pressure decrease linearly with increasing temperature in the examined temperature region of 25°C to the glass

transition temperatures. Thus, the enthalpy energy concept suggested above correlates the qualitative behavior of shear banding and yielding under pressure.

In order to quantitatively compare the experimental data with theoretical predictions, the following relation of the pressure dependency of energy densities was derived from eqs. (9), (10), and (11);

$$\left(\frac{\partial W}{\partial P}\right)_T = \frac{(1 - T\cdot\bar{\alpha})}{\bar{C}\cdot\bar{\rho}\ (Tg-T)}\ W(T,1) \tag{13}$$

A calculation was carried out assuming $\bar{C}_p$ = 0.36 (cal/gm°C)[37], $\bar{\rho}$ = 1.19 (gm/cm^3)[37], and Tg = 105°C[37], and $\bar{\alpha}$ = 2.3 x 10^{-4} (1/°C). From our experimental data at 23°C, W(T,1) = 0.18 (for shear banding) and 0.53 (cal/cm^3)(for yielding) were used. As shown in Table I, the agreement of the experimental values with the predicted ones is good especially for shear banding. Some additional observations on the enthalpy energy density and the correlation between the shear banding and yielding phenomena are in the DISCUSSION section.

Predictions of Young's Modulus and Fracture Stress

Young's modulus has been observed to increase substantially with increasing ambient hydrostatic pressure. Several attempts have been made to predict the pressure dependency of Young's modulus. Ainbinder et al.[7] introduced the relation between the modulus and pressure based on the finite elasticity theory derived by Murnaghan[20] and further developed by Birch[19]

$$E(P) = E_0 + 2(5 - 4\ \nu)P \tag{14}$$

where E(P) and E_0 are Young's moduli at pressure P and at atmospheric pressure, respectively, and ν is Poisson's ratio. However, they reported that eq.(14) did not fit with their experimental data for PMMA and other polymers. Later, Sauer et al.[16-18] proposed a similar relation, which was derived from the same references[19,20] using slightly different assumptions

$$E(P) = E_0 + 2(5 - 4\nu)(1 - \nu)P \tag{15}$$

and reported that the predicted values agreed well with the experimental data for PC and other polymers. On the contrary, Parry and Tabor[21] pointed out that the shear moduli for many polymers determined by means of a torsion pendulum under pressure did not support the finite strain elasticity theory. Thus, we still lack generally accepted theory for the pressure dependency of Young's modulus.

As demonstrated in Figure 6-a and 8, the eqs. (4) and (11) express with agreement the pressure dependencies of the shear band initiation stress and the energy density for shear band initiation. Therefore, these two equations may be utilized to construct a rather complex equation which predicts the pressure dependency of Young's modulus from $\varepsilon = 0$ to $\varepsilon = \varepsilon_{sb}$;

$$E(P) = \frac{\sigma_{sb}(P)}{\varepsilon_{sb}(P)} = \frac{\sigma_{sb}^{\,2}(P)}{2\,W_{sb}(P)} = \frac{(C^2+T^2) - (C-T)\{[(C+T)^2 + 12\,(C-T)P]^{1/2} - 6P\}}{4[W_{sb}(1) + \frac{1}{K}\,(1 - T\cdot\overline{\alpha})P]} \tag{16}$$

where $W_{sb}(1)$ is the value of energy density for shear band initiation at atmospheric pressure and the material constant K is calculated as 1.64×10^2 for PMMA from the experimental data. As expected, the predicted curve shows a

good agreement in the whole pressure range with the experimental values of Young's modulus as shown in Figure 9. In the figure, the theoretical line predicted from eq.(15) with $\nu = 0.38$ is also drawn for a comparison. The predicted line shows departure from the experimental data especially at higher pressure region.

The effect of pressure on the fracture stress in polymers has rarely been studied. Most reported experimental data for the fracture stresses under pressure are engineering stresses because of difficulty in observing the true fracture stress. The environmental effect on the fracture stress, not often noticed, is due to the surrounding pressure transmitting fluids. These difficulties, however, have been overcome in this study and an interesting correlation between the fracture stress and the applied pressure was observed. As already shown in Figures 1 and 2, the environmental effects on the mechanical behaviors of PMMA was significant. The effects of pressure on the fracture stresses for both unsealed and sealed specimens are shown in Figure 10, where the principal fracture stresses, $\sigma_f^1(P) = \sigma_f(P) - P$, are expresses as a function of applied pressure. The principal fracture stress for sealed specimens showed an almost constant positive value of 18 ksi in the whole ductile fracture region, while those for unsealed specimens decreased with pressure because of the environmental effect. This suggests that the ductile fracture under pressure occurs when the principal stress level of the specimen reaches a critical value irrespective of the applied pressure if there were no environmental effect. Furthermore, the relation $\sigma_f^1(P) = \text{const.}$ for sealed specimens implies that we can predict the ductile fracture stress at any pressure if the stress at one particular pressure such as atmospheric pressure is known[38].

DISCUSSION

The brittle to ductile transition in PMMA can be induced by simply changing temperature[39], by the application of a biaxial stress field[13,40], or by the superimposition of hydrostatic pressure as demonstrated in this study. In each case, however, different mechanisms have been proposed. Beardmore[39] suggested that the fracture and yield stresses have different temperature dependencies and that these stresses become equal at the brittle to ductile transition temperature. On the other hand, Sternstein and his co-workers[13,40] reported that the curves of the yield (shear yielding in their terms) stress and the craze initiation (normal stress yielding) stress intersect at the brittle to ductile transition point. Our results agree with Beardmore's phenomenalogical suggestion (see Fig. 5). In his suggestion, however, no specific mechanism at the microscopic level for the transition was implied. In this regard, our observation that the curves of the craze initiation stress and the shear band initiation stress intersect at the brittle to ductile transition point seems to be an essential and fundamental factor governing the transition phenonenon. This intersection mechanism of crazing and shear banding was previously suggested by us for the brittle to ductile transition observed in PS under pressure[4,41].

The yielding process in tensile deformation of PMMA is qualitatively quite similar to the results of Kramer[29] who studied in detail the compression deformation of PS. Both studies showed that the specimens in ductile fracture region exhibit shear bands accompanying the onset of non-linearity on the stress-strain curve: The stress maximum appears following the spread of the shear bands across the specimen width. We observed that the experimental data

for the shear banding agree much better with the values predicted from the non-linear pressure dependent von Mises criterion and the enthalpy energy theory than those for the yielding. This difference is probably due to the fact that the stress state in the specimen is uniform at the shear bands initiation stress, and then the stress distribution becomes increasingly inhomogeneous above the shear band initiation stress. Unfortunately, most previous studies on the yielding mechanism[42-45] seem to have been carried out using the yield stresses simply defined as the maximum stress point without considerations of the propagation process of shear band and the inhomogeneous nature of the stress distribution in the test specimen. For these reasons, further studies are needed to understand exactly the yielding process, although some relationship between the shear band initiation and the yield stresses has already been reported[30] and suggested in this work.

We have observed that the concept of the enthalpy energy density clearly explains the pressure dependency of the shear band initiation stress and fairly well that of yield stress. Starita and Keaton[46] proposed, similarly, an internal energy density concept for the yielding phenomenon. The mechanical energy necessary to cause glassy polymers to flow or yield can be directly related to the internal energy density U;

$$W(T) = \frac{b}{b'} \int_{T}^{Tg} \left(\frac{\partial U}{\partial T}\right)_p dT \simeq \frac{b}{b} \left(\bar{C}_p \cdot \bar{\rho} - \bar{\alpha} \cdot P\right)(T_g - T) \qquad (17)$$

where b and b′ are the fraction of thermal and mechanical energy available to overcome the activation energy for flow. This concept was further tested by Macosko and Brand[37] and reported to agree very well with the experimental data for five amorphous polymers from 25°C to the glass transition temperatures at atmospheric pressure. In their actual calculation of the

theoretical values, however, they employed the following approximated equation because $\bar{C}_p \cdot \bar{\rho} \gg \bar{\alpha} \cdot P$ at atmospheric pressure;

$$W(T) \simeq \frac{b}{b'} \bar{C}_p \cdot \bar{\rho} \, (Tg - T) \tag{18}$$

It is interesting to note that this eq. (18) is exactly eq. (9) at atmospheric pressure if $K = \frac{b'}{b}$. Therefore, these two concepts both successfully explain the experimental data at atmospheric pressure. However, we find that the internal energy density concept fails when the high pressure data are examined. The pressure dependency of the energy density predicted from the internal energy density concept may be expressed as

$$\left(\frac{\partial W}{\partial P}\right)_T = \frac{1}{K} \left(\bar{\beta} \cdot P - \bar{\alpha} \cdot T\right) \tag{19}$$

where $\bar{\beta}$ is the average value of compressibility in the pressure range 1 to P. This equation suggests that the pressure dependency of the energy density is not constant but a function of pressure, which does not agree with the experimental results shown in Figure 8. From these facts, we propose that the enthalpy energy density method can be applied in a wider range of temperature and pressure rather than the internal energy density method. A more fundamental basis for this enthalpy energy density concept might be found in the ideas of Goldstein[47,48] and Starita and Keaton[46].

Combination of the non-linear pressure dependent von Mises criterion and the enthalpy energy density theory for the shear band initiation stress enabled us to theoretically predict the pressure dependency of Young's modulus in PMMA. The non-linear pressure dependency of Young's modulus observed in PMMA is probably not due to a pressure-induced relaxation process since this

polymer has no mechanical relaxation maxima between the experimental temperature and about - 100°C. It is interesting to cite similar non-linear pressure dependent Young's moduli reported for several polymers by Sauer et al.[16-17]. They suggested that the observed non-linearity is due to the pressure-induced shift of a β or γ relaxation which are found at temperatures lower than room temperature at atmospheric pressure. Their experimental data on Young's modulus show that the pressure dependencies become "smaller" due to the pressure-induced shifting of mechanical relaxation, although this trend is the opposite to what might be expected. According to Paterson's work on various rubbers[49], Young's moduli increases drastically with pressure due to the pressure-induced shift of the glass transition. Moreover, Sauer's data show that the pressure dependency of Young's modulus exhibit non-linearity from atmospheric pressure in most polymers; even in polymers which can not be affected by the pressure-induced shifting of relaxation maxima.

In the preceding paper[4], we studied the mechanical behaviors of PS under pressure. The experimental results on PS have been further analyzed here, and we examined whether the enthalpy energy density theory on the shear banding phenomenon and the equation for the pressure dependency of Young's modulus proposed in this study are applicable for PS as well as PMMA. As shown in Figure 11, the shear band initiation stress in PS also shows a very good fit to the non-linear pressure dependent von Mises criterion in the whole pressure region. The enthalpy energy densities for the both shear banding and yielding exhibit a linear pressure dependency (Figure 12). Good agreement of the experimental values with the predicted values for the pressure dependency of the enthalpy energy density was obtained for shear

banding as shown in Table II. In the calculation of the theoretical values, the following thermodynamic values and experimental data were used; $\overline{C}_p$ = 0.30 (cal/gm°C)[50], $\overline{\rho}$ = 1.04 (gm/cm^3)[50], Tg = 95°C[41], T = 31°C, and W(T,1) = 0.13 (for shear banding) and 0.32 (cal/cm^3)(for yielding). Furthermore, we could accurately predict the pressure dependency of Young's modulus in PS as demonstrated in Figure 13. These facts convince us that the mechanisms and concepts derived from these studies on PMMA and PS can be applied to explain the mechanical behavior of other amorphous polymers under pressure.

CONCLUSIONS

Tensile experiments on PMMA under pressure showed the mechanical behavior of PMMA is strongly affected by the pressure transmitting fluid. When sealed specimens were tested in tension, PMMA has been shown for the first time to become ductile under hydrostatic pressure above 0.3 kb. Studies on sealed specimens enabled us to elucidate the mechanism of the brittle to ductile transition, to analyze the shear band initiation process thermodynamically, and to predict the values of shear band initiation stress and Young's modulus under pressure. The major conclusions of this study may be summarized as follows:

(1) Silicon oil used as a pressure transmitting fluid acts as a strong stress crazing and cracking agent for PMMA under pressure.

(2) The craze and shear band initiation stresses have different pressure dependent curves which intersect at the brittle to ductile transition pressure.

(3) The pressure dependency of the shear band initiation stress agrees well with a non-linear pressure dependent von Mises criterion.

(4) The energy density necessary for shear band initiation shows a linear pressure dependency. The enthalpy energy density theory predicts successfully this pressure dependency. The pressure and temperature effects on shear banding can also be correlated in terms of the enthalpy energy density.

(5) From the combination of the non-linear pressure dependent von Mises criterion and the enthalpy energy density theory the pressure dependency of Young's modulus can be predicted.

(6) Fracture in the ductile region occurs when the principal stress level of the specimen reaches a critical value irrespective of the applied pressure.

(7) The conclusions (1) - (6) listed above have been similarly shown to apply to PS.

ACKNOWLEDGEMENT

This research was generously supported by the Office of Naval Research.

REFERENCES

1. L. Holliday, J. Mann, G. A. Pogany, H. Pugh, and D.A. Gunn, Nature, 202, 381 (1964).

2. G. Biglione, E. Baer, and S. V. Radcliffe, in "Fracture 1969" Proceeding of the Second International Conference, Brington, 1969, edited by P. L. Pratt (Chapman and Hall, London, 1969).

3. H. Pugh, E. F. Chandler, L. Holliday, and J. Mann, Polymer Eng.,Sci., 11, 463 (1971).

4. K. Matsushige, S. V. Radcliffe, and E. Baer, J. Mater. Sci., in press.

5. S. K. Bhateja and K. D. Pae, Polymer Letter, 10, 531 (1972).

6. J. A. Sauer, S. K. Bhateja, and K. D. Pae, Third Inter-American Conference on Materials Technology; Rio de Janeiro, Brazil (1972).

7. S. B. Ainbinder, M. G. Laka, and I. Yu. Maiors, Polym. Mech., 1 (1), 50 (1965).

8. M. G. Laka and A. A. Dzenis, Polym. Mech., 3, 685 (1967).

9. W. I. Vroom and R. F. Westover, SPE J., 25, 58 (1969).

10. W. Whitney and R. D. Andrews, J. Polym. Sci., C16, 2981 (1967).

11. P. B. Bowden and J. A. Jukes, J. Mater. Sci., 3, 183 (1968).

12. J. C. Bauwens, J. Polym. Sci., A-2, 8,893 (1970).

13. S. S. Sternstein and L. Ongchin, A. C. S. Polym. Preprints,10, 1117 (1969).

14. R. Raghava, R. M. Caddell, and G. S. Y. Yeh , J. Mater. Sci., 8, 225 (1973).

15. F. Schleicher, Z. Agnew. Math. Mech., 6, 199 (1926).

16. D. R. Mears, K. D. Pae, and J. A. Sauer, J. Appl. Phys., 40, 4229 (1969).

17. J. A. Sauer, D. R. Mears, and K. D. Pae, Eur. Polym. J., 6, 1015 (1970).

18. J. A. Sauer, K. D. Pae, and S. K. Bhateja, J. Macromol. Sci. Phys., B8, 631 (1973).

19. F. Birch, J. Appl. Phys., 2, 279 (1938).

20. F. Murnaghan, Amer. J. Math., 59, 235 (1937).

21. E. J. Parry and D. Tabor, J. Mater. Sci., 9, 289 (1974).

22. S. Torp. R. G. C. Arridge, C. D. Armeniades, and E. Baer, Colston Conference on March 11, University of Bristol, England, April 2-4, 1974.

23. S. B. Newman and I. Wolock, J. Appl. Phys., 29, 49 (1958).

24. I. Wolock, J. A. Kies, and S. B. Newman, Fracture, Wiley, New York, 1959, p 250.

25. E. H. Andrews, Fracture in Polymers, Elsevier, New York, 1968.

26. P. Beardmore and J. Fellers, Mater. Sci. Eng., 5, 120 (1969/70).

27. J. Hoare and D. Hull, Phil. Mag., 26, 443 (1972).

28. I. Narisawa, J. Polym. Sci., A-2, 10, 1789 (1972).

29. E. J. Kramer, J. Macromol. Sci. Phys., B10(1), 191 (1974).

30. A. S. Argon, R. D. Andrews, J. A. Godrick, and W. Whitney, J. Appl. Phys., 39, 1899 (1968).

31. T. E. Brady and G. S. Y. Yeh, J. Appl. Phys., 42 , 4622 (1971).

32. T. E. Brady and G. S. Y. Yeh, J. Mater. Sci., 8, 1083 (1973).

33. M. Higuchi and H. Ishii, Repts. Res. Inst., Appl. Mech. Kyushu University, 16, 69 (1968).

34. C. B. Bucknell, D. Clayton, and W. E. Keast, J. Mater. Sci., 7, 1443 (1972).

35. S. Wellinghoff and E. Baer, to be published.

36. N. W. Tchoegl, Polym. Sci. Symp., 32, 239 (1971).

37. C. W. Macosko and G. J. Brand, Polym. Eng. Sci., 12, 444 (1972).

38. W. Whitney, Ph.D. thesis, MIT (1964).

39. P. Beardmore, Phil. Mag., 19, 389 (1969).

40. S. S. Sternstein and F. A. Myers, J. Macromol. Sci. Phys., B8(3-4), 539 (1973).

41. K. Matsushige, Ph.D. thesis, Case Western Reserve University, Cleveland (1975).

42. R. A. Cuckett, S. Rabinowitz, and I. M. Ward, J. Mater. Sci., 5, 909 (1970).

43. P. B. Bowden, J. A. Jukes, J. Mater. Sci., 7, 52 (1972).

44. A. Thierry, R. J. Oxborough, P. B. Bowden, Phil. Mag. 527 (1974).

45. T. E. Brady and G. S. Y. Yeh, J. Macromol. Sci., B9(4), 659 (1974).

46. J. M. Sterita and M. J. Keaton, SPE Technical Papers, 29 67 (1971).

47. M. Goldstein, J. Chem. Phys., 39, 3369 (1963).

48. M. Goldstein, J. Chem. Phys., 51, 3728 (1969).

49. M.S. Paterson, J. Appl. Phys., 35, 176 (1964).

50. R. H. Boundy and R. F. Boyer, eds., Stylene, Its Polymers, Copolymers and Derivatives, Reinhold Publishing, Co., New York, 1952.

FIGURE CAPTIONS

Fig. 1. Stress-strain curves for unsealed specimens at various pressures.

Fig. 2. Stress-strain curves for sealed specimens at various pressures.

Fig. 3. Stress-strain curve of PMMA specimen tested at 25°C and photographs of specimen at increasing tensile strains as seen in optical microscope.

Fig. 4. Stress-strain curve of PMMA specimen tested at 95°C and birefringent photographs with schematic figures of specimen at increasing tensile strains as seen in optical microscope.

Fig. 5. Pressure dependencies of craze initiation, shear band initiation, fracture and yield stress for sealed specimens. Arrow BD indicates the brittle to ductile transition.

Fig. 6. Comparisons of experimental results of shear band initiation stress (a) and yield stress (b) with theoretical values predicted from linear (eq.(3)) and non-linear pressure dependent von Mises criteria (eq.(4)).

Fig. 7. Typical stress-strain curve in ductile fracture region and energy densities for onset of shear banding and yielding.

Fig. 8. Pressure dependencies of energy densities for onset of shear banding and yielding.

Fig. 9. Comparison of experimental results of Young's modulus under pressure with theoretical values predicted from eq.(16) and by Sauer et al.[16-18] (eq. (15) with $\nu = 0.38$).

Fig. 10. Pressure dependencies of principal fracture stress in sealed and unsealed specimens. Arrow BD indicates the brittle to ductile transition.

Fig. 11. Comparison of experimental results of shear band initiation stress in PS with theoretical values predicted from linear (eq.(3)) and non-linear pressure dependent von Mises criteria (eq.(4)).

Fig. 12. Pressure dependencies of energy densities for onsets of shear banding and yielding in PS.

Fig. 13. Comparison of experimental results of Young's modulus under pressure in PS with theoretical values predicted from eq.(16) and Sauer et al.[16-18] (eq. (15) with $\nu = 0.33$).

Table I. Comparison of experimental results for pressure dependency of energy densities for shear banding and yielding with theoretical values predicted from eq.(13).

Table II. Comparison of experimental results for pressure dependency of energy densities for shear banding and yielding in PS with theoretical values predicted from eq. (13).

	Shear Banding	Yielding
Experimental ($X10^{-3}$)	5.0	17
Theoretical ($X10^{-3}$)	4.9	14
$\frac{\text{Exper. - Theo.}}{\text{Exper.}}$ (%)	2	18

Table I. Comparison of experimental results for pressure dependency of energy densities for shear banding and yielding with theoretical values predicted from eq.(13).

	Shear Banding	Yielding
Experimental ($X10^{-3}$)	6.3	11
Theoretical ($X10^{-3}$)	6.1	15
$\frac{\text{Exper. - Theo.}}{\text{Exper.}}$ (%)	3	-36

Table II. Comparison of experimantal results for pressure dependency of energy densities for shear banding and yielding in PS with theoretical values predicted from eq.(13).

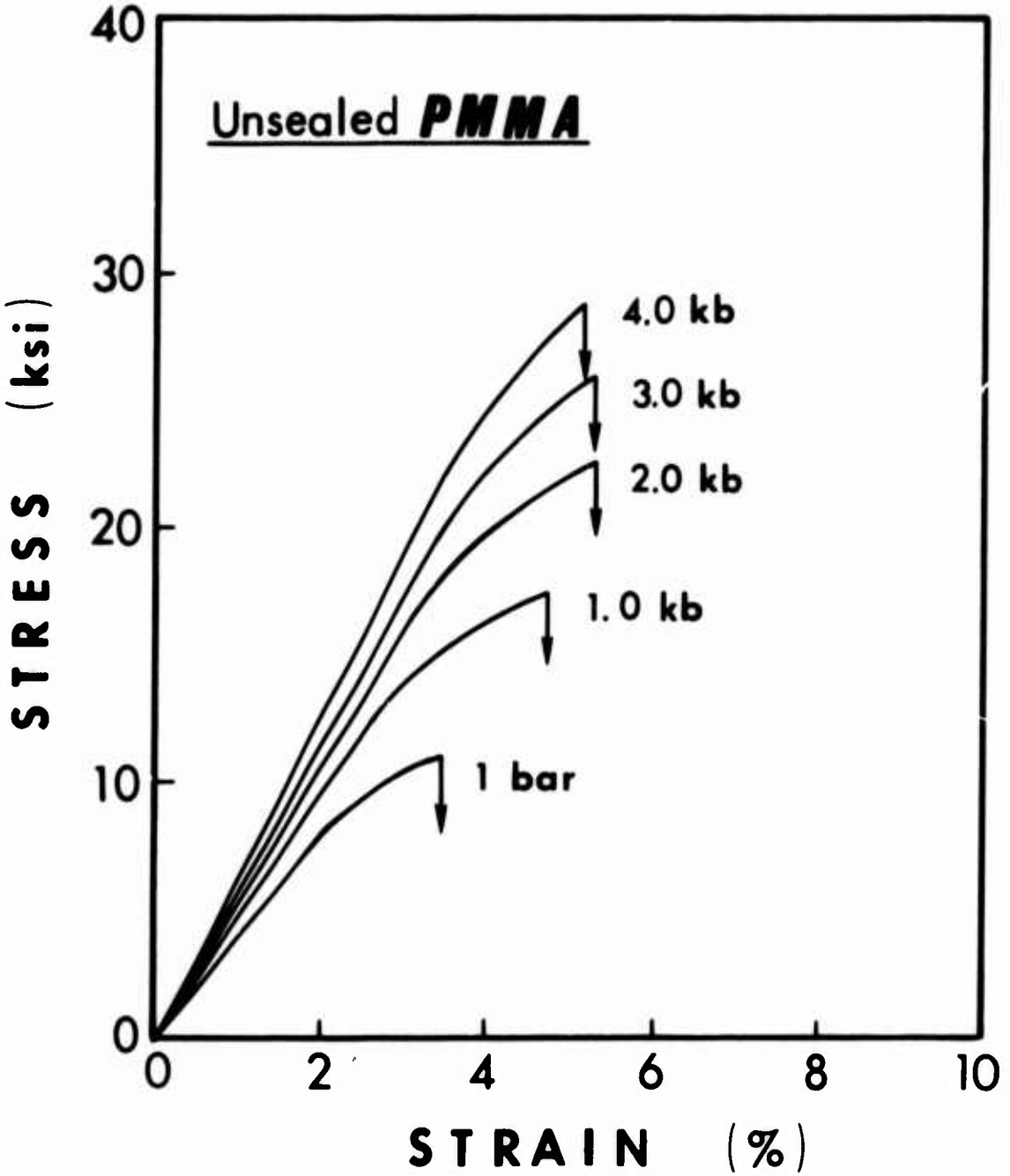
Unsealed PMMA
4.0 kb
3.0 kb
2.0 kb
1.0 kb
1 bar
STRESS (ksi)
STRAIN (%)
0
10
20
30
40
0
2
4
6
8
10

FIGURE 1

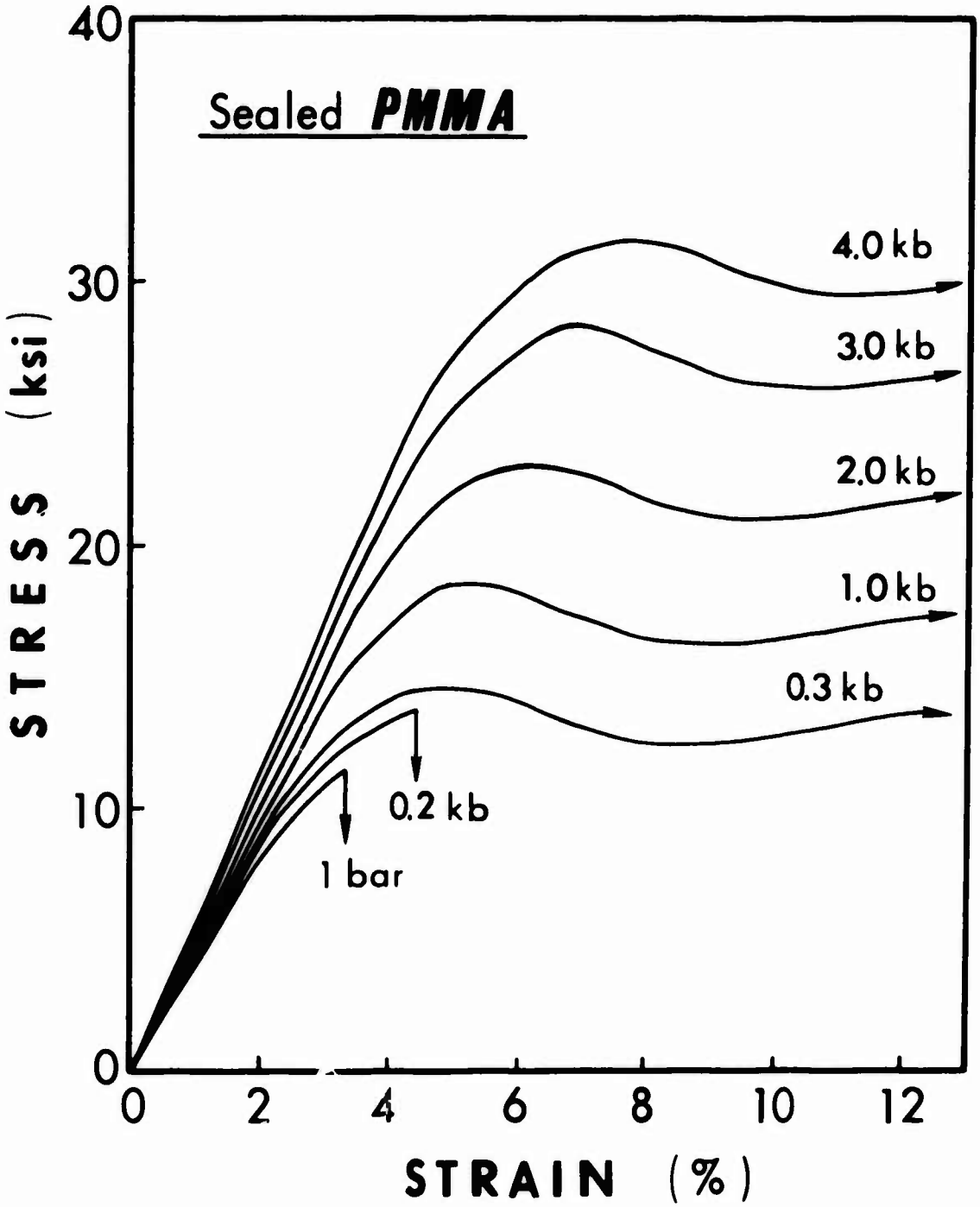
Sealed PMMA
4.0 kb
3.0 kb
2.0 kb
1.0 kb
0.3 kb
0.2 kb
1 bar
STRESS (ksi)
STRAIN (%)
0
10
20
30
40
0
2
4
6
8
10
12

FIGURE 2

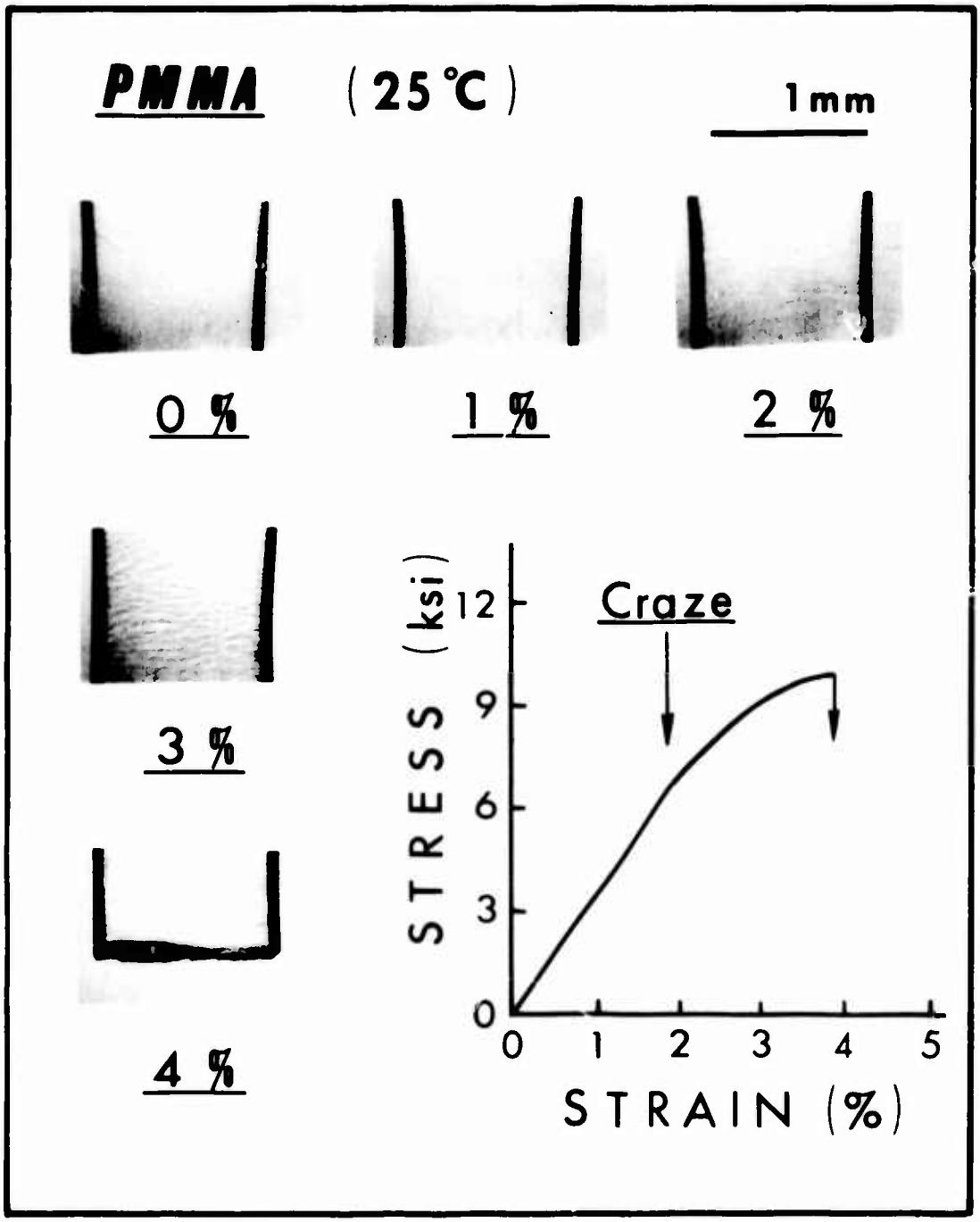

FIGURE 3

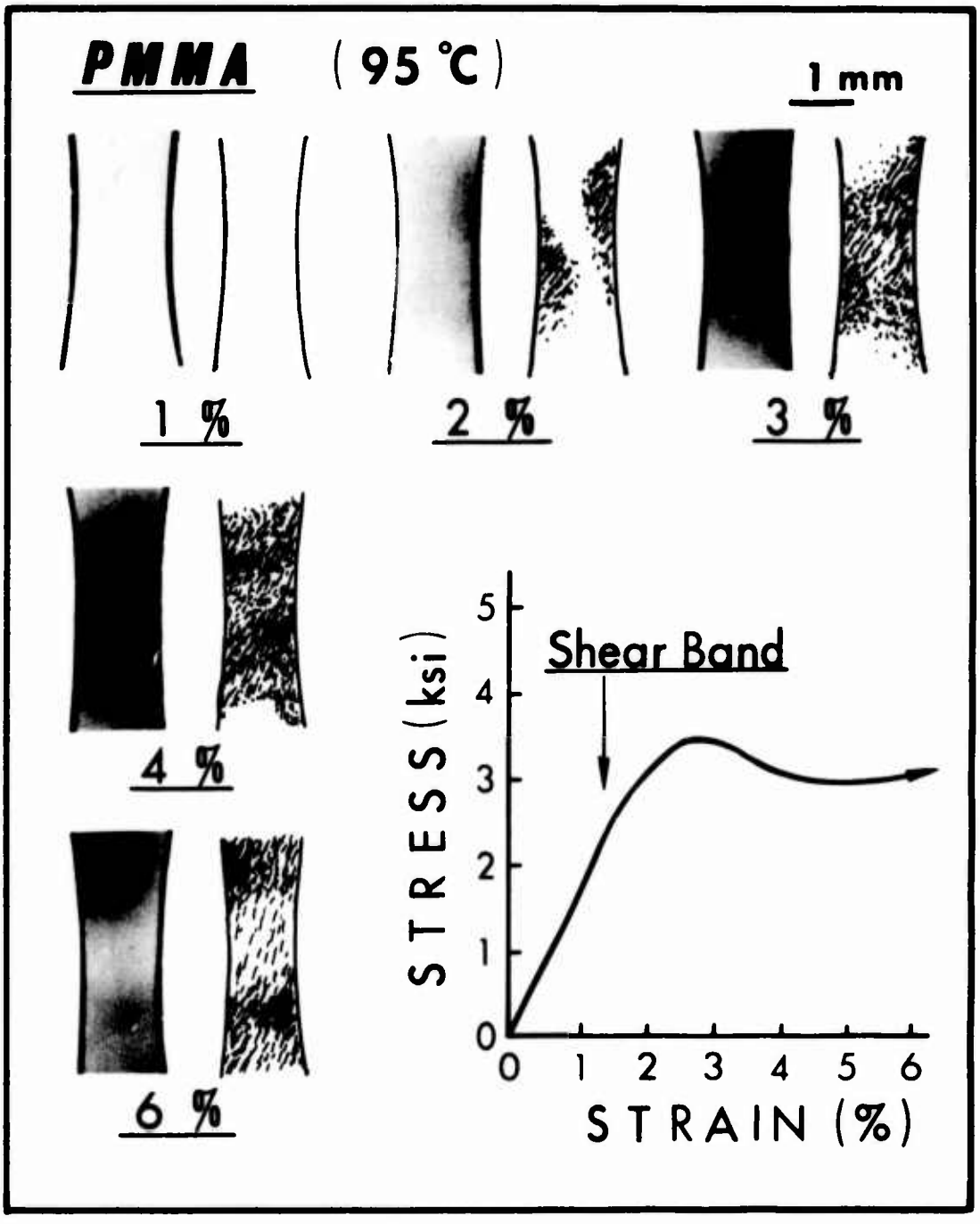

FIGURE 4

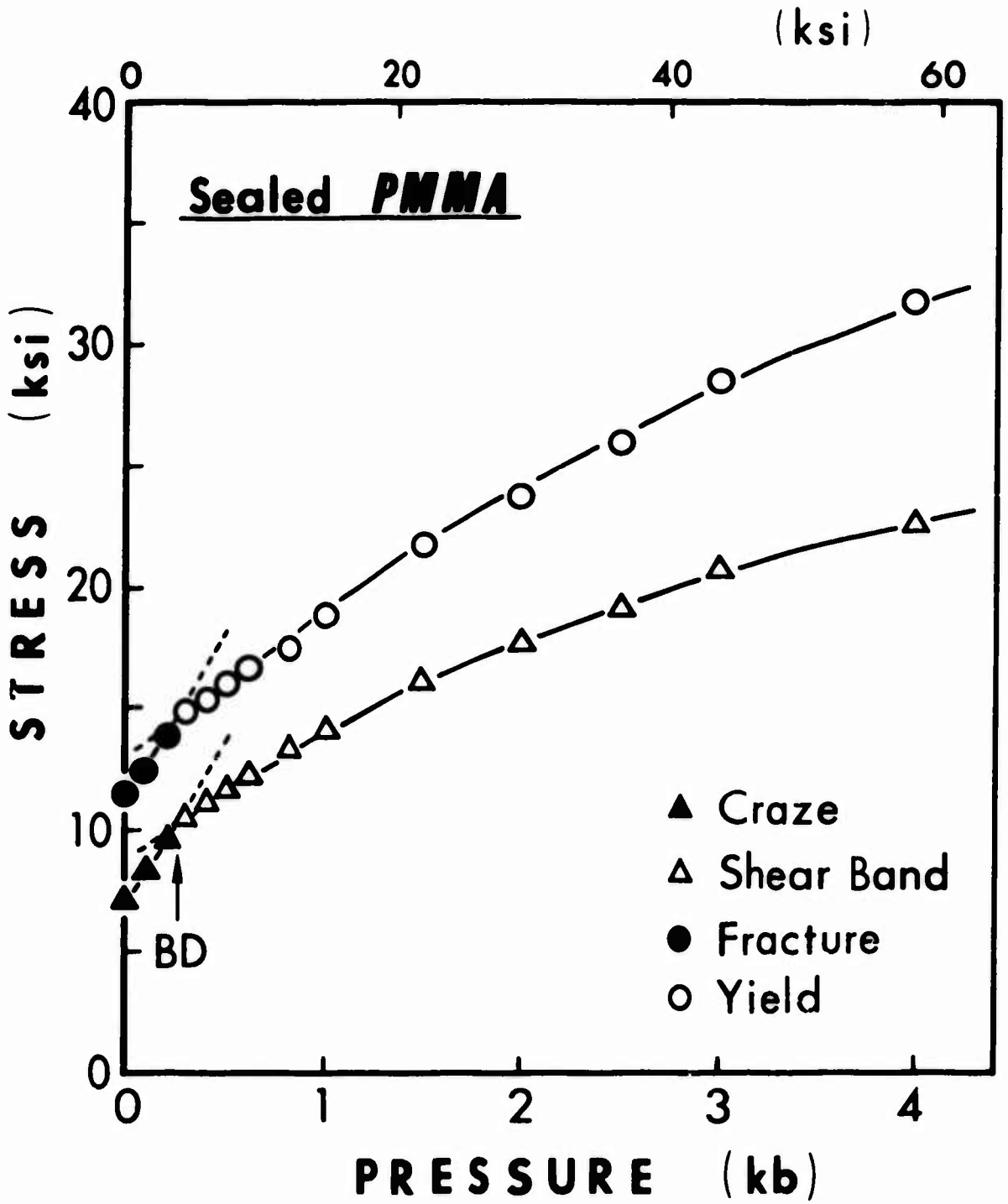
(ksi)
0
20
40
60
40
30
20
10
0
Sealed PMMA
STRESS (ksi)
BD
▲ Craze
△ Shear Band
● Fracture
○ Yield
0
1
2
3
4
PRESSURE (kb)

FIGURE 5

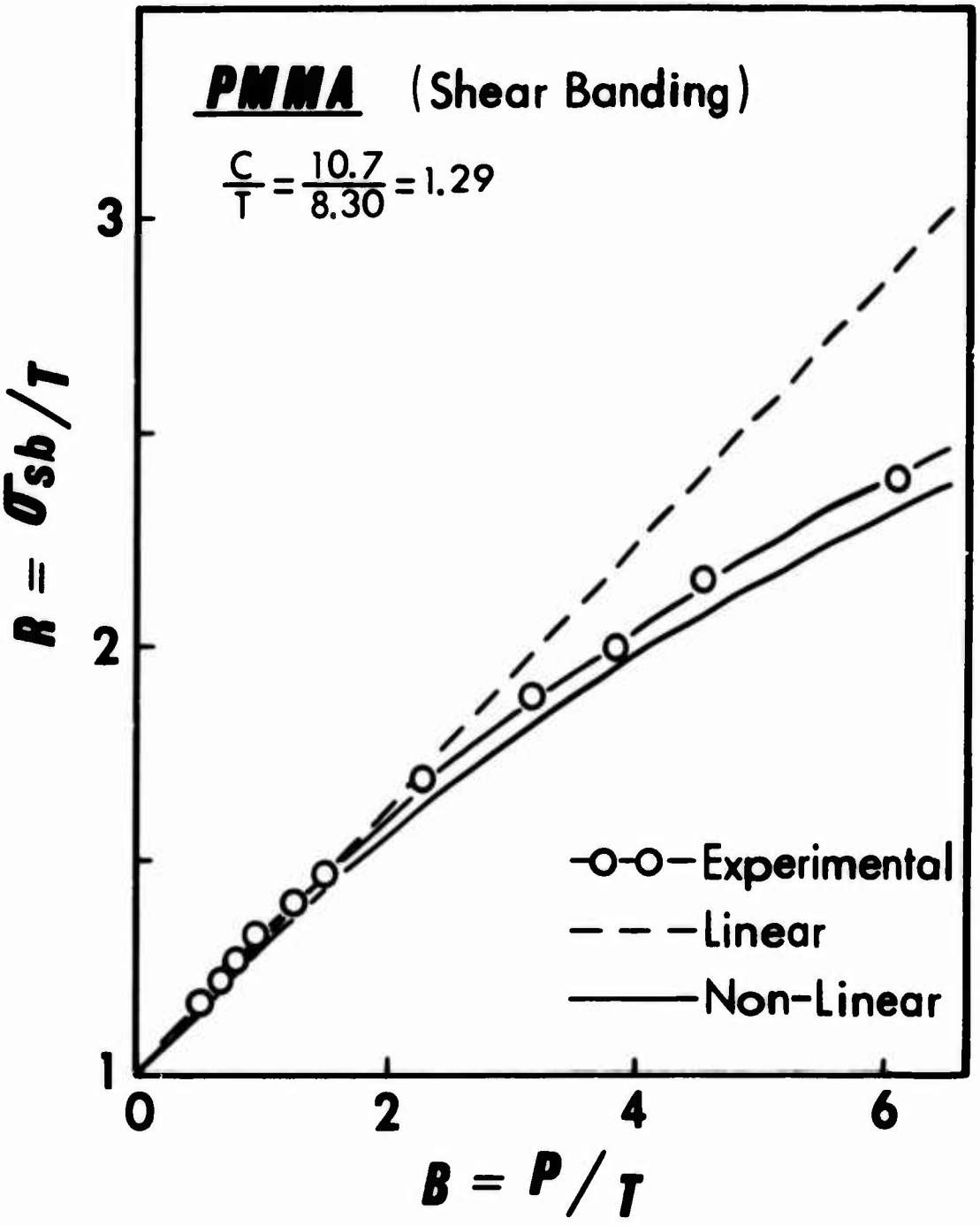
PMMA (Shear Banding)
C/T = 10.7/8.30 = 1.29
R = σsb/T
B = P/T
3
2
1
0
2
4
6
Experimental
Linear
Non-Linear

FIGURE 6-(a)

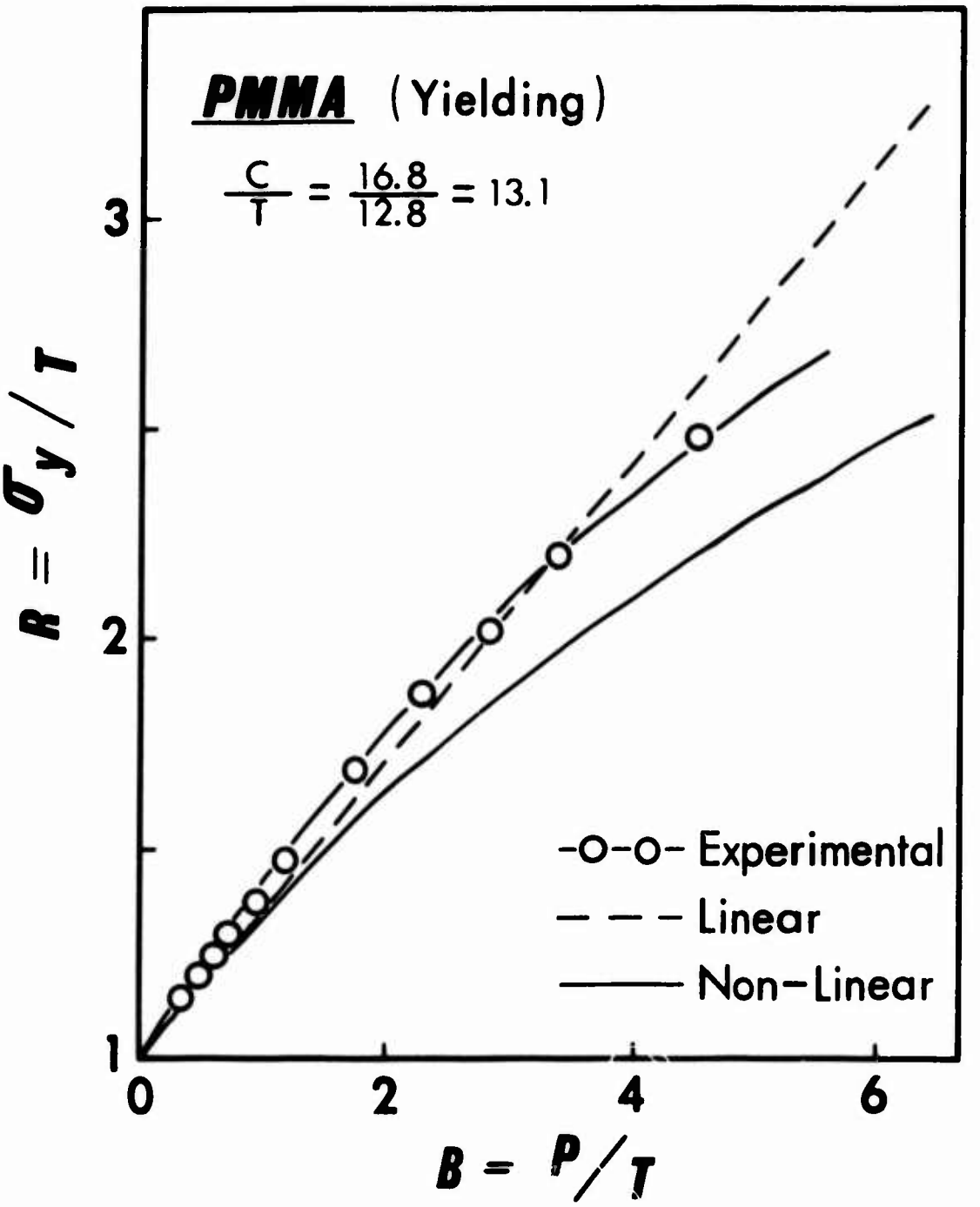
PMMA (Yielding)
C/T = 16.8/12.8 = 13.1
R = σy / T
B = P / T
0
2
4
6
1
2
3
-O-O- Experimental
— — — Linear
——— Non-Linear

FIGURE 6-(b)

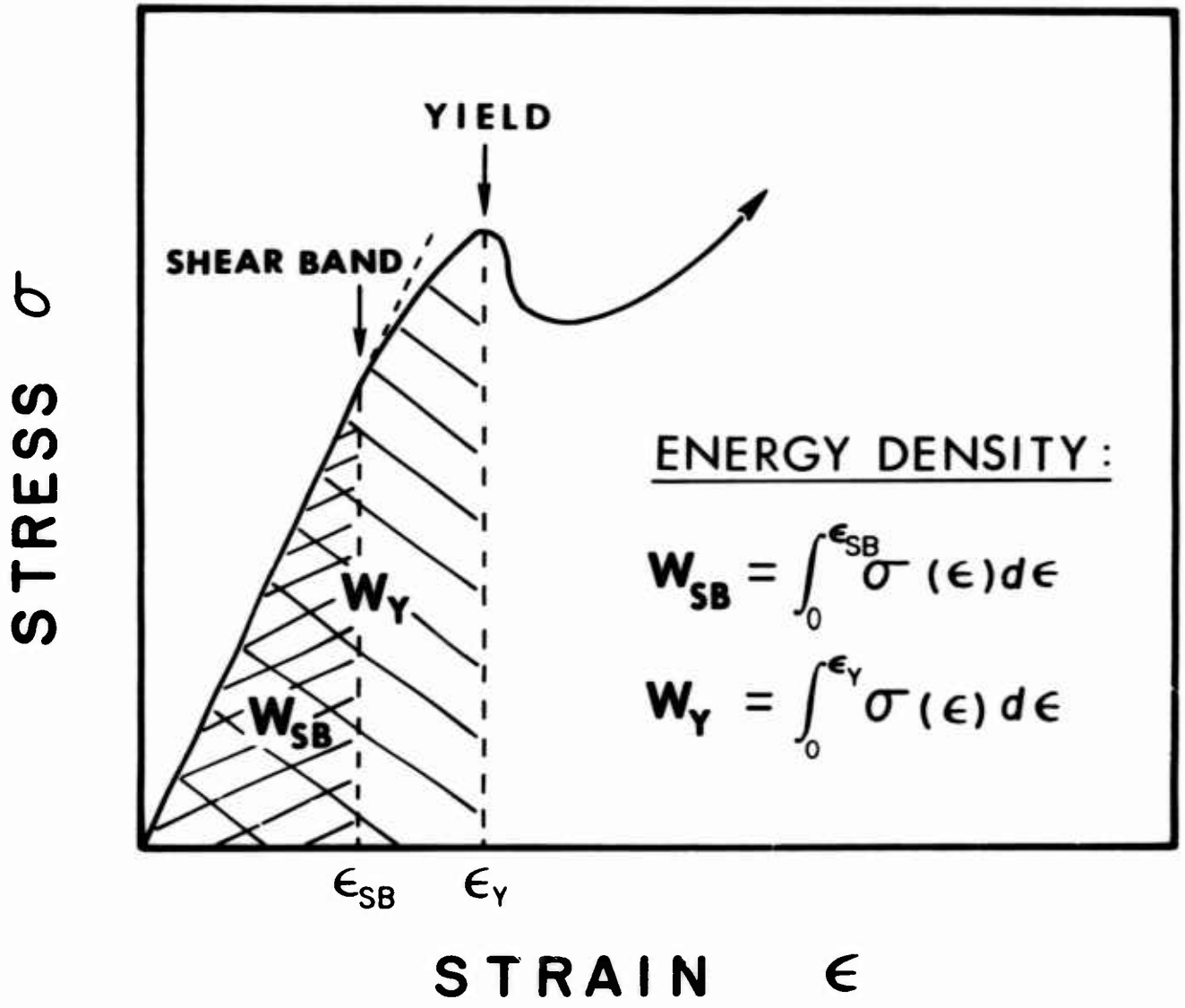
YIELD
SHEAR BAND
STRESS σ
ENERGY DENSITY:
$W_{SB} = \int_0^{\epsilon_{SB}} \sigma(\epsilon) d\epsilon$
$W_Y = \int_0^{\epsilon_Y} \sigma(\epsilon) d\epsilon$
W_Y
W_{SB}
ϵ_{SB}
ϵ_Y
STRAIN ϵ

FIGURE 7

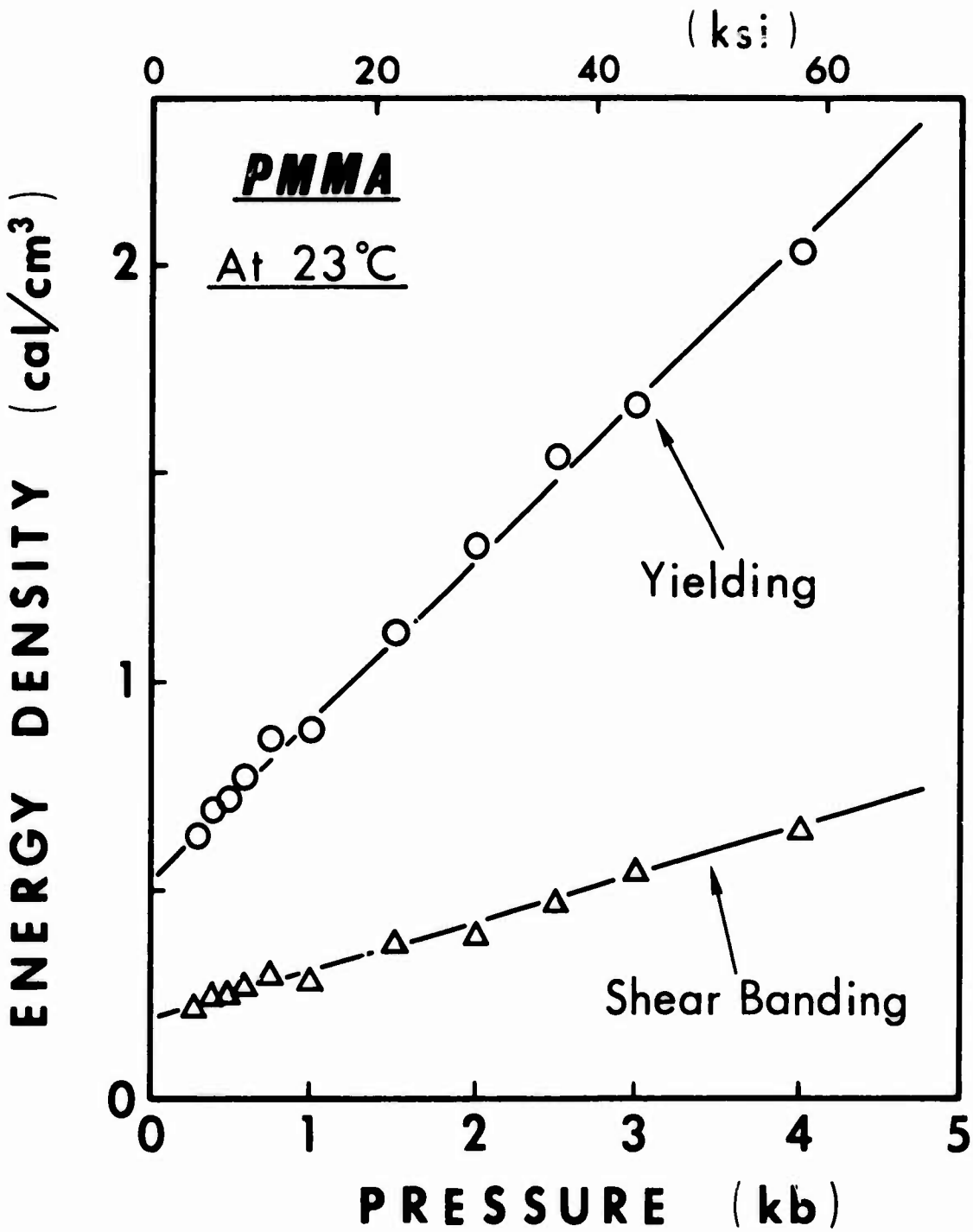
(ksi)
0
20
40
60
PMMA
At 23°C
2
1
0
ENERGY DENSITY (cal/cm³)
Yielding
Shear Banding
0
1
2
3
4
5
PRESSURE (kb)

FIGURE 8

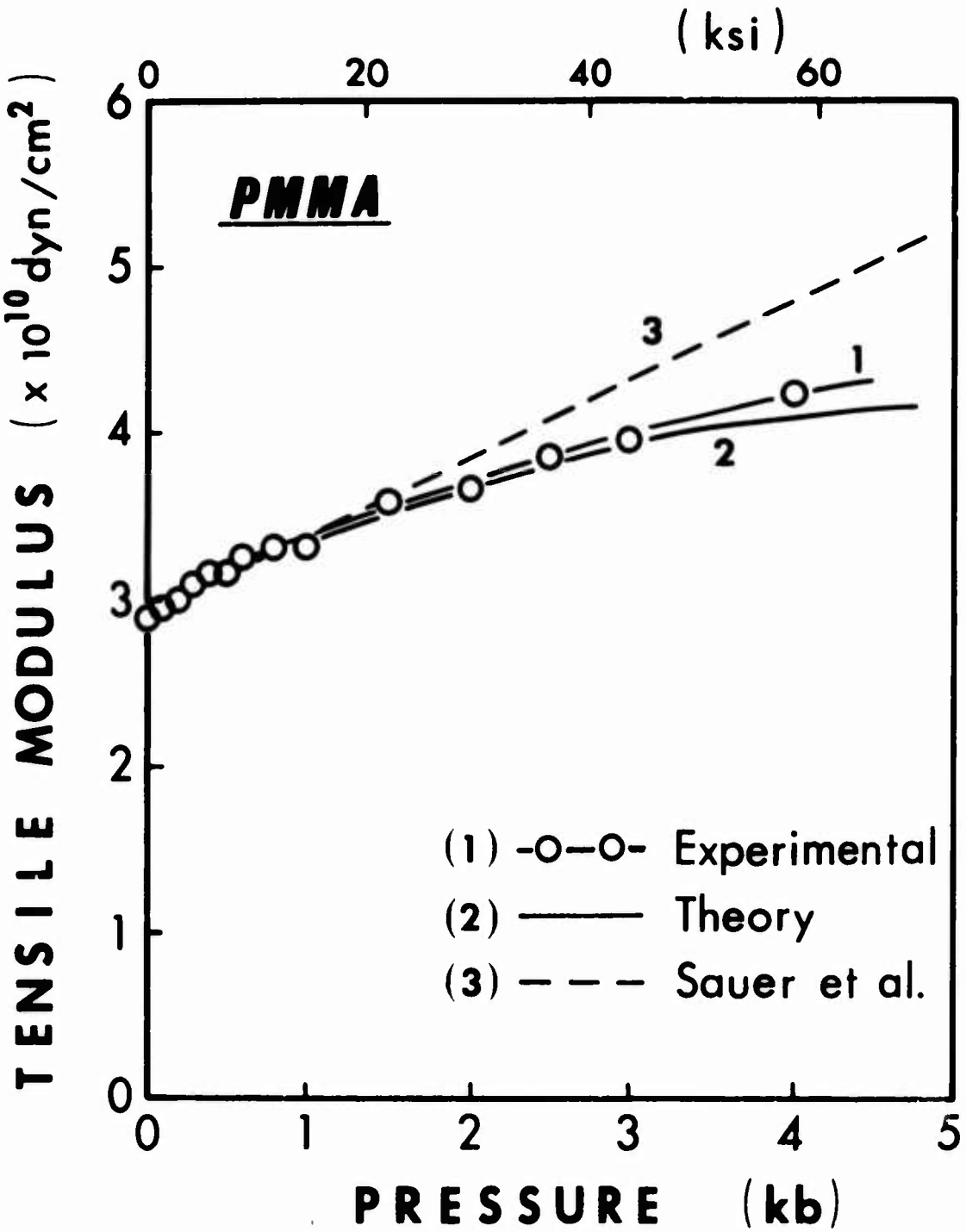
(ksi)
0
20
40
60
6
5
4
3
2
1
0
TENSILE MODULUS (x 10^10 dyn/cm^2)
PMMA
3
1
2
(1) -o-o- Experimental
(2) ——— Theory
(3) – – – Sauer et al.
0
1
2
3
4
5
PRESSURE (kb)

FIGURE 9

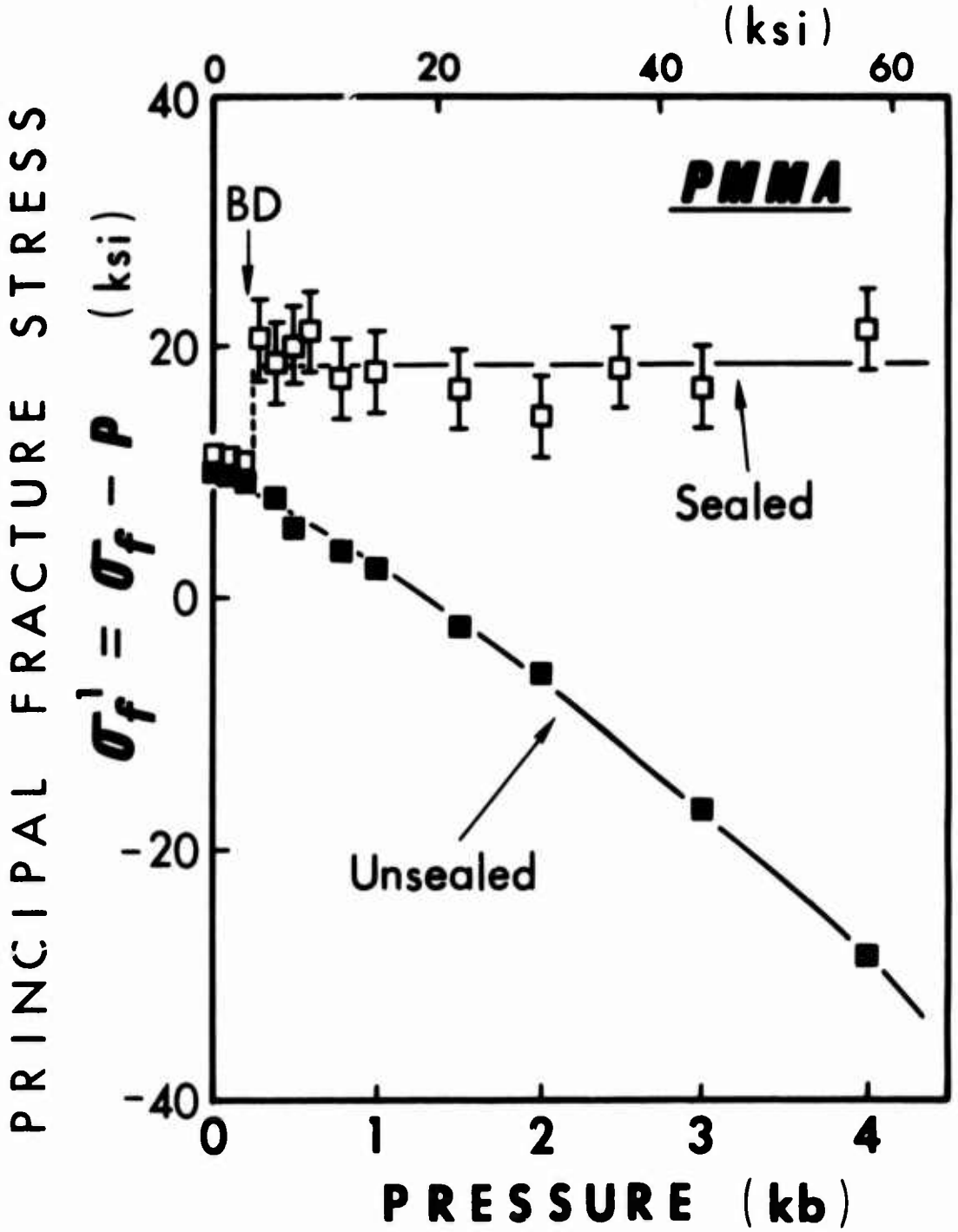
(ksi)
0
20
40
60
40
20
0
-20
-40
PMMA
BD
Sealed
Unsealed
PRINCIPAL FRACTURE STRESS
$\sigma_f' = \sigma_f - P$ (ksi)
0
1
2
3
4
PRESSURE (kb)

FIGURE 10

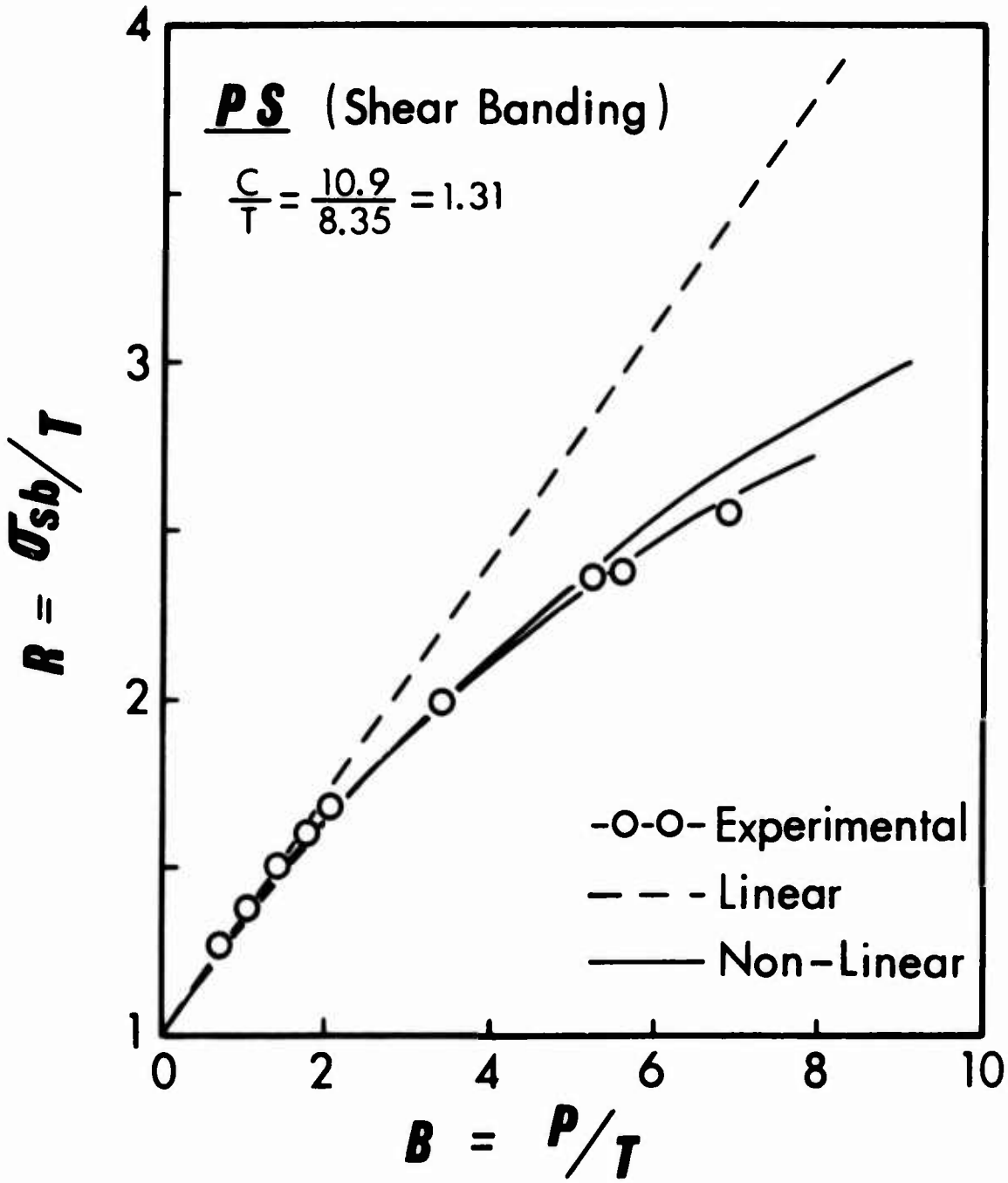
PS (Shear Banding)
C/T = 10.9/8.35 = 1.31
R = σsb/T
B = P/T
-o-o- Experimental
- - - Linear
—— Non-Linear
0
2
4
6
8
10
1
2
3
4

FIGURE 11

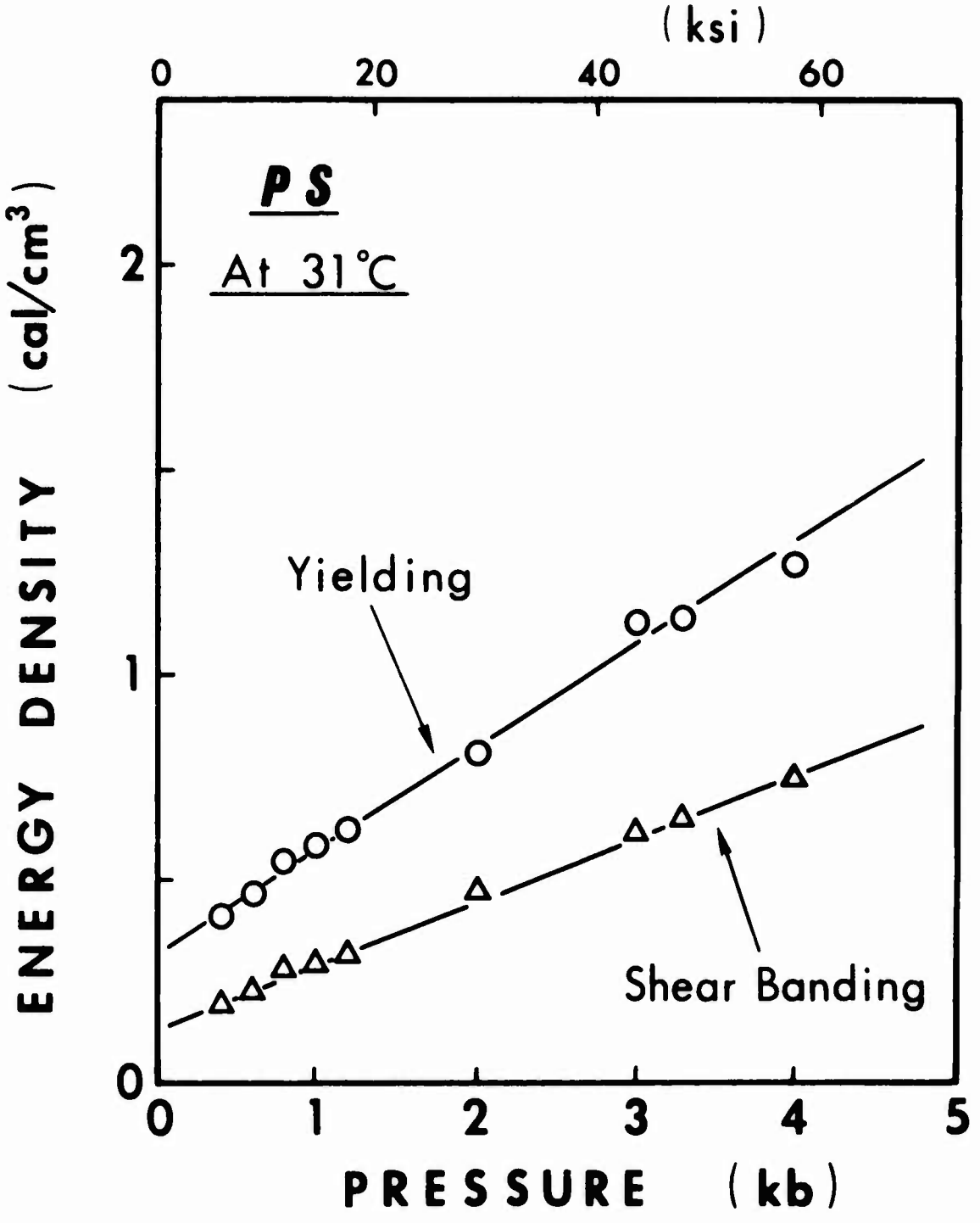
(ksi)
0
20
40
60
PS
At 31°C
ENERGY DENSITY (cal/cm³)
2
1
0
Yielding
Shear Banding
0
1
2
3
4
5
PRESSURE (kb)

FIGURE 12

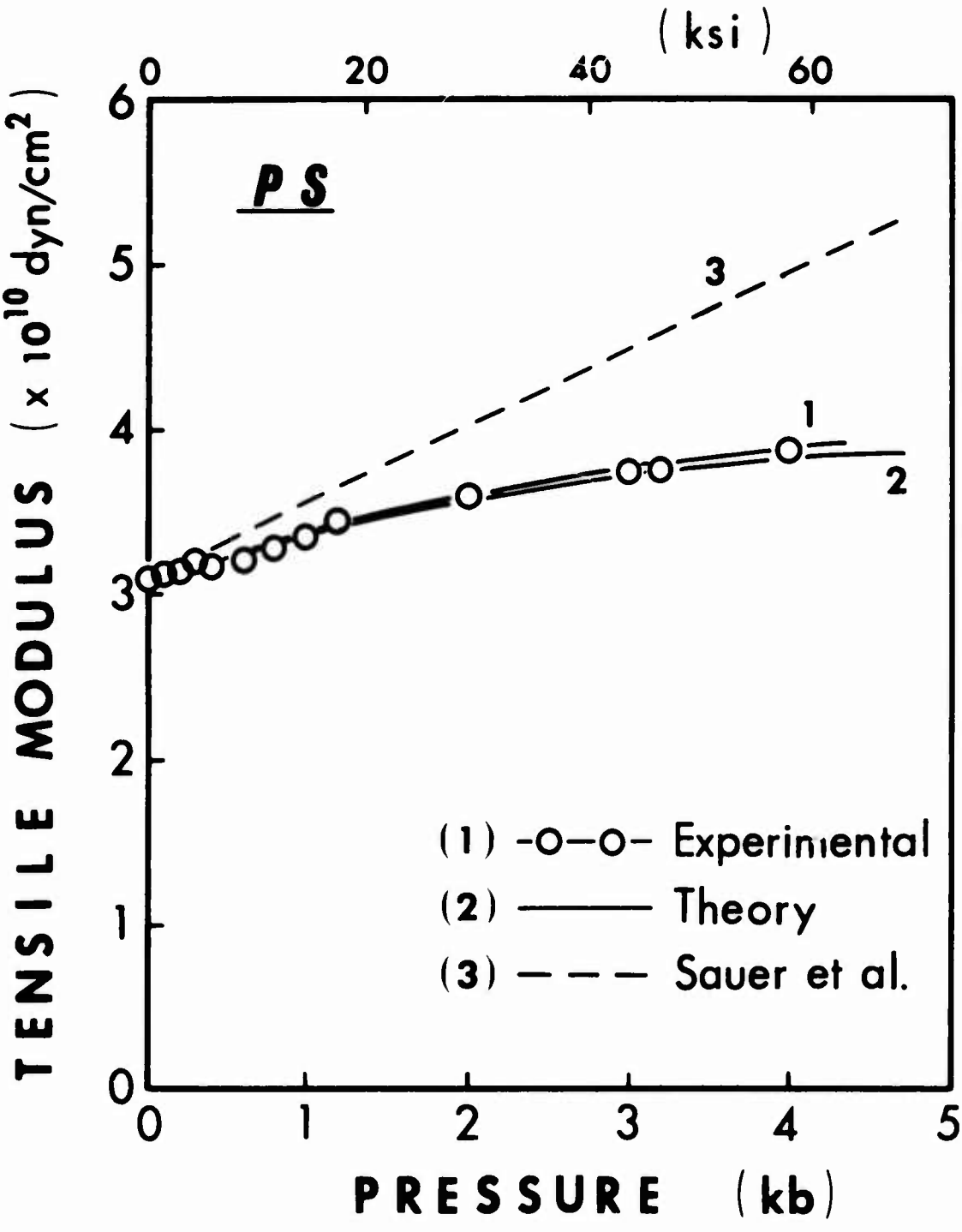
(ksi)
0
20
40
60
6
5
4
3
2
1
0
PS
3
1
2
TENSILE MODULUS (x 10^10 dyn/cm^2)
(1) -o-o- Experimental
(2) ——— Theory
(3) — — — Sauer et al.
0
1
2
3
4
5
PRESSURE (kb)

FIGURE 13